The result, 16.76, which we had derived originally in 1979 landed in the plateau region established by the dynamical procedures.

We consider that the application of an extrapolation procedure - by using a wedge-shaped single-crystal specimen or by tilting a parallel-sided specimen (Lawrence & Mathieson, 1976) or by estimating the level of extinction (first approximation) from the profile curve (Mackenzie & Mathieson, 1979) - is advisable to establish properly a zero-extinction limit. That there may also be a scale-factor modifier for the γ-ray data is a possibility which cannot be excluded. However, to authenticate this possibility, the applicability of the Darwin transfer relationship requires to be explored more closely, experimentally as well as theoretically.

We are grateful to Drs G. Kemister and P. J. Lloyd for their careful reading of the text in relation to band-structure calculations.

References

ARLINGHAUS, F. J. (1967). *Phys. Rev.* **153**, 743-750.
BAGAYOKO, D., LAURENT, D. G., SINGHAL, S. P. & CALLAWAY, J. (1980). *Phys. Lett. A*, **76**, 187-190.
COURTHS, R. & HÜFNER, S. (1984). *Phys. Rep.* **112**, 53-171.
DARWIN, C. G. (1914). *Philos. Mag.* **27**, 315-333.
EKARDT, H., FRITSCHE, L. & NOFFKE, J. (1984). *J. Phys. F*, **14**, 97-112.
FOX, A. G. & FISHER, R. M. (1988). Unpublished.
International Tables for X-ray Crystallography (1974). Vol. IV, Table 2.2*D*. Birmingham: Kynoch Press. (Present distributor Kluwer Academic Publishers, Dordrecht).
JENNINGS, L. D., CHIPMAN, D. R. & DEMARCO, J. J. (1964). *Phys. Rev.* **135**, 1612-1615.
KULDA, J. (1987). *Acta Cryst.* A**43**, 167-173.
LAWRENCE, J. L. & MATHIESON, A. MCL. (1976). *Acta Cryst.* A**43**, 1002-1004.
MACDONALD, A. H., DAAMS, J. M., VOSKO, S. H. & KOELLING, D. D. (1982). *Phys. Rev. B*, **25**, 713-725.
MACKENZIE, J. K. & MATHIESON, A. MCL. (1979). *Acta Cryst.* A**35**, 45-50.
MACKENZIE, J. K. & MATHIESON, A. MCL. (1984). *Aust. J. Phys.* **37**, 651-656.
MATHIESON, A. MCL. (1979). *Acta Cryst.* A**35**, 50-57.
NITTONO, O., YAMAGISHI, H. & NAGAKURA, S. (1979). *J. Appl. Cryst.* **12**, 141-146.
SCHNEIDER, J. R. (1974). *J. Appl. Cryst.* **7**, 541-546.
SCHNEIDER, J. R. (1976). *J. Appl. Cryst.* **9**, 394-402.
SCHNEIDER, J. R. (1977). *Acta Cryst.* A**33**, 235-243.
SCHNEIDER, J. R., HANSEN, N. K. & KRETSCHMER, H. (1981). *Acta Cryst.* A**37**, 711-722.
SCHNEIDER, J. R., PATTISON, P. & GRAF, H. A. (1979). *Nucl. Instrum. Methods*, **166**, 1-19.
SMART, D. J. & HUMPHREYS, C. J. (1980). *Inst. Phys. Conf. Ser.* No. 52, 211-214.
SNOW, E. C. (1968). *Phys. Rev.* **171**, 785-789.
SPACKMAN, M. A. (1986). *Acta Cryst.* A**42**, 271-281.
TABBERNOR, M. A., FOX, A. G. & FISHER, R. M. (1990). *Acta Cryst.* A**46**, 165-170.
TAKAMA, T. & SATO, S. (1982). *Philos. Mag.* B**45**, 615-626.
TEMKIN, R. J., HENRICH, V. E. & RACCAH, P. M. (1972). *Phys. Rev. B*, **6**, 3572-3581.
WAKOH, S. & YAMASHITA, J. (1971). *J. Phys. Soc. Jpn*, **30**, 422-427.
WOOD, J. H. (1967). In *Energy Bands in Metals and Alloys*, edited by L. H. BENNETT & J. T. WABER, pp. 43-63. New York: Gordon & Breach.

Acta Cryst. (1992). A**48**, 236-243

Extinction in Mixed Magnetic and Nuclear Reflections. A Study of the Magnetic Structure of $TbAlO_3$ using Neutron Polarimetry and Integrated Intensity Measurements

BY P. J. BROWN, V. NUNEZ AND F. TASSET

Institut Laue-Langevin, BP 156X, 38042 Grenoble, France

AND J. B. FORSYTH

Isis Science Division, Rutherford Appleton Laboratory, Chilton, Didcot, Oxon OX11 0QX, England

(*Received* 2 *August* 1991; *accepted* 19 *September* 1991)

Abstract

The magnetic structure of $TbAlO_3$ single crystals has been studied using zero-field neutron polarimetry and neutron integrated intensity measurements. The results of neither kind of measurements could be understood using a simple model for extinction in the rather good untwinned crystals that were used. To explain the results the Becker-Coppens extinction model [Becker & Coppens (1974). *Acta Cryst.* A**30**, 129-147] has been extended to the case where several magnetic domains occur within one block of the nuclear structure. The consequences for both the integrated intensities and the scattered polarizations have been calculated and it has been shown that the model provides a consistent interpretation of both

0108-7673/92/020236-08$03.00

sets of measurements. The results for the magnetic structure are in good agreement with a previous powder diffraction study.

1. Introduction

In recent years we have been developing the technique of general polarization analysis to study absolute magnetic configurations in single crystals of antiferromagnetic materials. In particular, the rotation of neutron polarization by the imaginary part of the interference term between magnetic and nuclear scattering, first noted by Blume (1963), can determine the sense in which the moment points with respect to a polar crystallographic environment. The symmetry requirements for this term to be non-zero are precisely those required for the existence of magnetoelectricity, *viz* the propagation vector of the magnetic structure must be zero and, if the magnetic point group includes a centre of symmetry, this must be combined with time reversal (see, for example, Cox, 1974).

In previous experiments we have studied the systems Cr_2O_3, $LiCoPO_4$ and $LiNiPO_4$. In Cr_2O_3 a unique sense for the direction of rotation of the polarization was found, suggesting that one orientation of the moment with respect to the sense of the polar (trigonal) axis is more stable than the other (Tasset, Brown & Forsyth, 1988). In $LiCoPO_4$ and $LiNiPO_4$, on the other hand, the rotation of the polarization was detected primarily as depolarization of the beam. Such behaviour indicates almost equal populations of right- and left-turning domains, which must therefore have nearly equal energies in these compounds.

We have now chosen to re-examine the magnetic structure of $TbAlO_4$, since it provides an opportunity to study the effect of a polar environment on the absolute-moment direction of a rare-earth ion. In the early stages of the experiment, however, when only unpolarized-beam integrated intensity data had been measured, it became clear that the magnetic scattering was much less extinguished than the nuclear scattering from the rather good single-crystal sample. We now describe an extension to the Becker–Coppens (1974) treatment of extinction which has enabled us to model not only these observations but also the polarization analysis data. The magnetic structure of $TbAlO_3$ is found to be in good agreement with that proposed by Mareschal, Sivardière, De Vries & Bertaut (1968) on the basis of neutron powder data.

2. The structure of $TbAlO_3$

$TbAlO_3$ is a member of a series of isostructural compounds ABO_3, where A is a trivalent transition-metal ion or aluminium and B is a trivalent rare-earth ion, which have a distorted perovskite structure and space group *Pbmn*. The cell dimensions of $TbAlO_3$ are $a = 5.229$, $b = 5.308$ and $c = 7.415$ Å at ambient temperature (Wells, 1970). The atomic positions are Tb in 4(*c*) $(x, y, \frac{1}{4})$, Al in 4(*b*) $(\frac{1}{2}, 0, 0)$, O1 in 4(*c*) and O2 in a general position 8(*a*). The positional parameters of the isostructural $DyAlO_3$ were determined in a room-temperature powder study by Bidaux & Meriel (1968) and these have been used as starting values for the structure refinements.

The compound was found to undergo an antiferromagnetic transition at 3.95 K, accompanied by the appearance of magnetoelectricity (Mercier & Cursoux, 1968). In the magnetic structure determined by Mareschal *et al.* (1968) the Tb moments lie in the mirror plane perpendicular to [001] and make angles ±36° to [100] as shown in Fig. 1. Since the Tb-moment direction is polar, the configuration in Fig. 1(*a*) is distinguishable from that in Fig. 1(*b*), in which all the moment directions are reversed.

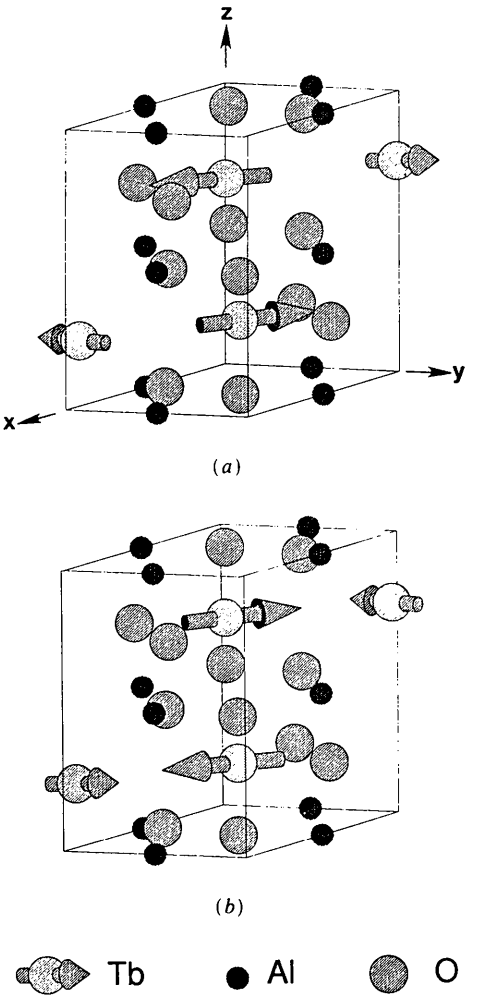

Fig. 1. The magnetic structure of $TbAlO_3$: (*a*) and (*b*) represent the two different 180° domains.

3. Experimental

3.1. *Integrated intensity measurements*

Two optically transparent untwinned crystals of $TbAlO_3$ were available. They had been grown by Dr R. C. C. Ward at the Clarendon Laboratory, Oxford University and used previously in the magnetic susceptibility and specific heat studies of Wells (1970). The crystals were in the form of right prisms of nearly rectangular cross section, the prism faces being {110} with an interfacial angle of 89.5°. The normal-beam diffractometer D15 at the Institut Laue–Langevin (ILL) was used to check the crystal quality and to mount the larger of the two crystals ($3\times3\times5$ mm) with its long c axis aligned parallel to the ω axis of the diffractometer. A set of integrated intensities was measured with the sample at ambient temperature and a neutron wavelength of 1.176 Å. Reflections of the form $hk0$ were measured out to the limit ($2\theta = 130°$) of the machine and these were supplemented by a few reflections ($hk1$) from the first layer. After averaging the intensities of equivalent reflections, we obtained a unique set of 85 measured structure factors. The crystal was subsequently placed in a standard ILL 'Orange' cryostat and a limited data set containing reflections in layers 0, 1 and 2 with $(\sin\theta)/\lambda < 0.5$ Å^{-1} was collected, first with the crystal in the antiferromagnetic phase at 1.5 K and then at 12 K just above the antiferromagnetic-to-paramagnetic transition. In both sets equivalent intensities were averaged, yielding a unique set of 45 non-zero structure factors measured at 12 K and 58 at 1.5 K: the difference in number being due to those magnetic reflections which are systematically absent in the nuclear space group.

3.2. *Polarization analysis measurements*

These measurements were carried out using the zero-field polarimeter Cryopad on the IN20 polarized-beam triple-axis spectrometer at the ILL. The principles and operation of the Cryopad have been fully described elsewhere by Tasset (1989) and Brown, Nunez, Tasset, Forsyth & Radhakrishna (1990). In short, it allows both the input neutron-beam polarization to be set at any desired angle and the magnitude and direction of the polarization in the diffracted beam to be found under the control of a PDP11/73 computer. The diffracting sample is kept in a field-free region and its temperature can be maintained in the range 2.0–315 K. Although the Cryopad makes it possible to set the input polarization **P** to any desired angle, it is convenient from the point of view of subsequent analysis to make scans in which **P** is varied in the three principal planes defined by the axes x parallel to the scattering vector $\boldsymbol{\kappa}$, z vertical and y making a right-handed set. In view of the time available, the $TbAlO_3$ measurements were restricted to the six 'cardinal directions' parallel to $\pm x$, $\pm y$ and $\pm z$.

The first set of measurements was made on the smaller of the two crystals which had edges of 2.4, 2.8 and 2.8 mm parallel to $[1\bar{1}0]$, [110] and [001], respectively. The crystal was mounted so that $[1\bar{1}0]$ was accurately aligned parallel to the ω (z) axis of the Cryopad. Reflections of at least two forms of six inequivalent hhl reflections 111, 112, 113, 220, 221 and 001 were then measured with the sample held at a nominal temperature of 2.5 K. Some difficulty was experienced in keeping this temperature constant over long periods and data taken at temperatures outside the range 2.1–2.8 K were subsequently rejected. Our measurements of the sublattice magnetization reported in § 9 show that its variation within this temperature range would not introduce an unacceptable drift in the direction of the output polarization. The temperature dependence of the scattered polarization was then measured for the 112 reflection as the sample was heated above its Néel point.

Two further sets of data were collected, one from the larger crystal with its [001] mounting in which forms of the inequivalent reflections 110, 120, 210, 220, 230 and 140 were measured at 2.5 K. These measurements were completed with a temperature scan of the 140 reflection. Finally, the smaller crystal was remounted about [010] and forms of the 101, 103, 105, 201 and 303 measured at 2.5 K.

In all, a total of 540 different determinations of the scattered polarization were made in a period of 3 d, which included the time taken to refill the helium in the cryostat and to exchange samples.

4. Preliminary analysis of the integrated intensity data

Least-squares refinements of the integrated intensities recorded at room temperature and at 12 K showed that the $TbAlO_3$ crystal exhibited severe extinction as might be expected from such a good untwinned sample. The extinction was modelled using the Becker–Coppens (1974) formalism and good agreement between the observed and calculated nuclear structure factors was obtained from a least-squares refinement of the room-temperature data set starting from the parameters for $DyAlO_3$. Both these parameters and the refined values for $TbAlO_3$ are reported in Table 1. With a domain radius of 7.3 μm primary extinction within the mosaic blocks could be appreciable and the primary-extinction correction given by Becker & Coppens (1974) was included in a subsequent refinement. This refinement gave a significantly worse fit to the data and smaller values of both the domain radius and mosaic spread. The result of the smaller domain radius is that the correction for primary extinction becomes negligible in comparison with that for secondary extinction. We have

Table 1. *Parameters obtained from the least-squares refinements of the structure of* $TbAlO_3$

The numbers in parentheses give the standard deviations of the parameters; if no standard deviation is given the corresponding parameter was fixed in the refinement.

Parameter		300 K	12 K
Tb	x	−0.0096 (4)	−0.0086 (11)
	y	0.0429 (3)	0.0444 (10)
	B (Å^{-2})	0.02 (9)	0.01
Al	B (Å^{-2})	0.11 (13)	0.06
O1	x	0.0768 (6)	0.0792 (13)
	y	0.4832 (4)	0.4829 (14)
	B (Å^{-2})	0.23 (9)	0.12
O2	x	−0.2892 (3)	−0.2891 (9)
	y	0.2888 (2)	0.2893 (8)
	z	0.0427	0.0419 (16)
	B (Å^{-2})	0.16 (9)	0.08
Domain radius (μm)		7 (4)	7.3
Mosaic spread (mrad)		0.35 (10)	0.35
Scale		122 (5)	121 (1)
Number of reflections		62	45
R factor on F (%)		2.7	3.7

Table 2. *Parameters obtained from refinements of the magnetic structure of* $TbAlO_3$

The positional and thermal parameters were fixed to those obtained for the nuclear structure at 12 K. The columns labelled $F(a)$, $F(b)$ and $F(c)$ refer to refinements based on integrated intensity measurements using different extinction models: (a) total 1.5 K intensity modelled by Becker–Coppens (B-C) with domain radius and scale values from the 12 K nuclear refinement; (b) 1.5 K magnetic intensity modelled by B-C with scale from 12 K nuclear refinement but allowing the domain radius to refine; (c) total 1.5 K intensity modelled by extended B-C theory. The column labelled PA gives the results of the final refinement based on the scattered polarizations.

Parameter		$F(a)$	$F(b)$	$F(c)$	PA
Tb Moment (μ_B)		16.7 (5)	7.8 (3)	8.25	8.31 (11)
φ (°)		32 (2)	36 (1)	37 (1)	30.5 (6)
Domain radii (μm)	r_N	7.3	-	7.3	7.3
	r_I	-	-	2.6 (2)	1.82 (10)
	r_M	-	0.9 (2)	0.9 (2)	0.46 (5)
Mosaic spread (mrad)		0.35	0.35	0.35	0.35
Overlap		-	-	0.23 (16)	0.14 (3)
Number of observations		58	58	58	540
R factor on F (%)		6.5	8.0	5.6	-

therefore made the assumption that primary extinction within the mosaic blocks can be neglected.

The 12 K data set is restricted to relatively low momentum transfers and the temperature factors are therefore not well determined. We have therefore fixed them to physically realistic values (one half of the values obtained at room temperature). The extinction parameters obtained from the room-temperature data were retained and the scale factor and atomic positions of the 12 K data set were refined. The results are also given in Table 1. No significant difference is found between the positional parameters at 300 and 12 K although the latter have not been obtained with great precision. The fact that the two scale factors are identical shows that the cryostat introduces negligible absorption.

The scale factor, extinction and structural parameters of the 12 K refinement were then introduced as fixed parameters in a least-squares refinement of the magnetic structure from the 1.5 K data set. The magnetic structure model used was that of Mareschal *et al.* (1968) which has two adjustable parameters: the magnetic moment of terbium and its inclination φ to the a axis in the ab plane. In this and all subsequent magnetic calculations the dipole approximation to the form factor of Tb,

$$f_{Tb}(\kappa) = \langle j0\rangle_{Tb} + \tfrac{1}{3}\langle j2\rangle_{Tb},$$

was used. In this equation $\langle j0\rangle_{Tb}$ and $\langle j2\rangle_{Tb}$ are the radial integrals for the free Tb^{3+} ion calculated by Freeman & Desclaux (1979). The result of the refinement, which is given in column $F(a)$ of Table 2, was unsatisfactory in that it yielded the unphysical value of $17\mu_B$ for the magnetic moment of Tb; it was concluded that either the proposed magnetic structure was incorrect or that there was something fundamentally wrong with the treatment of extinction. We were led to adopt the latter conclusion for two reasons. Firstly, if it is assumed that nuclear and magnetic scattering are equally extinguished, the order of magnitude of the magnetic scattering can be estimated by according the same scale and extinction factors to nuclear and magnetic reflections which occur at similar scattering angles and have approximately the same intensity. It was immediately clear that this assumption leads to experimental magnetic scattering factors greater than could be obtained for any magnetic structure with only $9\mu_B$ per Tb atom. For instance, if the integrated intensity measured for the purely magnetic 201 reflection is scaled using the nuclear scale and corrected for extinction using the nuclear extinction model it yields an experimental magnetic structure factor of about 13.5×10^{-12} cm. After dividing by the form factor this corresponds to $48\mu_B$ for four Tb ions. Secondly, it was found that, if a set of magnetic intensities was deduced by direct subtraction of the reflection intensities measured at 12 K from those measured at 1.5 K, these data were consistent with the magnetic structure obtained from powder diffraction allowing a smaller domain radius for the magnetic scattering but using the scale factor obtained from the extinction-corrected nuclear refinement. The results of this refinement are listed in column $F(b)$ of Table 2. We have therefore been led to the conclusion that the magnetic scattering is much less extinguished than is the nuclear scattering.

5. A model for extinction in mixed magnetic nuclear reflections

Before a proper analysis of the results of the polarization analysis experiments can be made, it is necessary to develop a model for the extinction

process for the case where both magnetic and nuclear scattering occur in the same Bragg reflections. In order to explain the results described above, this model must allow a different amount of extinction for the two types of scattering. Also, to be applicable to polarization analysis data, it must predict the polarization of the scattered beam. Although the $TbAlO_3$ crystals are reasonably perfect, it has been shown that their behaviour is far from dynamical; the model should therefore describe secondary rather than primary extinction. The parameters in the Becker-Coppens treatment of extinction are the angular width of the mosaic block distribution, the mosaic spread, and the size the blocks themselves, the domain radius. It is not easy to imagine, within this model, how a different mosaic spread can apply to magnetic and nuclear scattering since the lattice, within which the defects giving rise to such blocks occur, is the same for magnetic and nuclear scattering. On the other hand, it is quite reasonable to postulate different domain radii, since a region of crystal which is perfect as far as its nuclear structure is concerned may contain several different magnetic domains.

When a crystal undergoes a transition to an ordered magnetic structure there is a possibility that different parts of the crystal will belong to different magnetic domains. The number of different types of domain depends on the relative symmetries of the paramagnetic and ordered phases, and domain formation may introduce local lattice distortions if symmetry is lost in the transition. In a magnetic structure like that of $TbAlO_3$ in which magnetic and nuclear scattering occur in the same reflections (propagation vector zero), domains of the 180° type can always occur. These domains are regions of crystal in which the moments of atoms in the same positions with respect to the origin of the unit cell are oppositely directed. Such domains introduce no lattice deformation whilst, across the boundary between two such domains, the relative phase of the potentials for nuclear and magnetic scattering of neutrons changes by 180°.

The domain radius enters into the Becker-Coppens extinction model in two ways: firstly, its size gives the primary-extinction correction and, secondly, it fixes the width of the rocking curve of a single mosaic block. The full width α of the rocking curve in this model has the form

$$\alpha^2 = [(\lambda / r \sin\theta)^2 + (1/2g)^2]^{-1}.$$

The extinction parameters obtained in the nuclear refinement indicate that, over most of the angular range, the width of the rocking curve is dominated by the mosaic spread, *i.e.* $r(\sin\theta)/\lambda > 2g$. It is quite possible therefore that if the size of the 180° magnetic domains is much less than that of the mosaic blocks, the width of the rocking curve for magnetic scattering could be much larger than that for nuclear scattering and consequently the magnetic scattering would show less extinction. To obtain more than a qualitative picture, and in particular to determine the effect of extinction on the scattered polarization, it is necessary to develop in more detail the form of the reflection curve from a mosaic block containing several magnetic domains.

In the kinematical approximation the elastic scattering cross section $\partial\sigma/\partial\omega$ is proportional to the Fourier transform (FT) of the static pair correlation function $g(r)$. In the present case the appropriate correlation function is

$$g(\mathbf{r}) = \int [\rho_N(\mathbf{R}+\mathbf{r}) + \boldsymbol{\rho}_M(\mathbf{R}+\mathbf{r})][\rho_N(\mathbf{R}) + \rho_M(\mathbf{R})]\, \mathrm{d}R^3$$

where $\rho_N(\mathbf{r})$ and $\rho_M(\mathbf{r})$ are respectively the nuclear and magnetic scattering densities. The FT of $g(\mathbf{r})$ is the sum of three terms: one nuclear, one magnetic and one nuclear-magnetic interference term. Each term is the FT of a convolution of two scattering densities and thus is given by the product of their FTs. The nuclear scattering density for one mosaic block can be written as the product of a shape function $S_N(\mathbf{r})$, which is zero outside the block and unity within it, and the ideal nuclear structure. Its FT, $T_N(\boldsymbol{\kappa})$, for $\boldsymbol{\kappa}$ near to a reciprocal-lattice vector $\mathbf{h}$, is $D_N(\boldsymbol{\kappa}-\boldsymbol{\eta})N(\mathbf{h})$ where $D_N(\boldsymbol{\kappa})$ is the FT of the shape function and $N(\mathbf{h})$ the nuclear structure factor for the reflection with scattering vector $\mathbf{h}$. Suppose the magnetic scattering density within the mosaic block arises from n domains whose shape is described by the function $S_M(\mathbf{r})$, but which are arranged randomly within the block described by $S_N(\mathbf{r})$ so that there is no correlation between the position and type of the domains. The magnetic scattering density then has the form

$$\rho_M(\mathbf{r}) = \sum_d S_M(\mathbf{r}-\mathbf{r}_d)\mathbf{U}_d(\mathbf{r})$$

where $\mathbf{U}_d(\mathbf{r})$ is the ideal magnetic structure of domain d. If the magnetic structure factor for domain d is $\mathbf{M}_d(\mathbf{h})$, then the FT of the magnetic scattering density is $\sum_d \mathbf{M}_d(\mathbf{h}) D_M(\mathbf{k}-\mathbf{h}) \exp(i\boldsymbol{\kappa}\cdot\mathbf{r}_d)$. The products giving the scattering cross section as a function of the deviation $\boldsymbol{\varepsilon} = \boldsymbol{\kappa} - \mathbf{h}$ are then:
for the nuclear scattering only:

$$|D_N(\varepsilon)|^2 |N(\mathbf{h})|^2;$$

for pure magnetic scattering:

$$|D_M(\varepsilon)|^2 \sum_d \alpha_d |\mathbf{M}(\mathbf{h})|^2;$$

for the interference term:

$$2\,\mathrm{Re}\, D_N(\varepsilon) D_M(\varepsilon) N(\mathbf{h}) \sum_d \alpha_d \mathbf{M}(\mathbf{h});$$

with α_d being the fraction of the crystal volume belonging to domain d. In fact the magnetic part of the scattering is not simply dependent on the magnetic structure factors, but depends on its component $\mathbf{Q}$

perpendicular to **h** and also on the neutron polarization. Nevertheless, these three equations show the form of the scattering curve near to a Bragg reflection and this is illustrated schematically in Fig. 2. The scattering due to the pure nuclear, the pure magnetic and the interference terms are represented as rectangular functions of different widths. Within the angular range of the sharpest distribution there are three contributions to the scattering: the whole of the nuclear part, a fraction ω_1/ω_2 of the interference scattering and a fraction ω_1/ω_3 of the magnetic scattering. In the range of ε between $\omega_1/2$ and $\omega_2/2$ there are contributions from just the magnetic and interference terms, and in the outermost region only magnetic scattering contributes.

6. Application of the model to the analysis of extinction in the magnetic scattering data

The assumption we have made in analysing our data is that the three ranges of the scattering curve described above contribute independently to the measured intensities and polarizations. We also assume that the Becker–Coppens formalism can be applied to each range separately and that they share a common mosaic spread but have different domain radii (r_N, r_M, r_I). The ratios between the three domain radii depend upon the average number n of magnetic domains in a mosaic block: the simplest assumptions lead to $r_N/r_M = n^{1/3}$ and $r_N/r_I = n^{1/6}$. Expanding the expressions for the magnetic scattering into the form which gives their dependence on $\mathbf{Q}(\mathbf{h})$ and the neutron polarization $\mathbf{P}$ (Blume, 1963) and writing N for $N(\mathbf{h})$ and $\mathbf{Q}$ for $\mathbf{Q}(\mathbf{h})$, the kinematical cross sections for the three ranges are

$$(\partial\sigma/\partial\omega)_1 = NN^* + \sum_d \alpha_d\{f(\mathbf{P}\cdot\mathbf{Q}_d N^* + \mathbf{P}\cdot\mathbf{Q}_d^* N) + f^2[\mathbf{Q}_d\cdot\mathbf{Q}_d^* - i\mathbf{P}\cdot(\mathbf{Q}_d\times\mathbf{Q}_d^*)]\}$$

$$(\partial\sigma/\partial\omega)_2 = \sum_d \alpha_d\{(1-f)(\mathbf{P}\cdot\mathbf{Q}_d N^* + \mathbf{P}\cdot\mathbf{Q}_d^* N) + (f-f^2)[\mathbf{Q}_d\cdot\mathbf{Q}_d^* - i\mathbf{P}\cdot(\mathbf{Q}_d\times\mathbf{Q}_d^*)]\}$$

$$(\partial\sigma/\partial\omega)_3 = \sum_d \alpha_d\{(1-f)^2 \times[\mathbf{Q}_d\cdot\mathbf{Q}_d^* - i\mathbf{P}\cdot(\mathbf{Q}_d\times\mathbf{Q}_d^*)]\}$$

where f measures the degree to which the reflection curves for nuclear and magnetic scattering overlap. The intensity I_s scattered into these three ranges is related to the kinematical intensity I_k by $I_{si} = I_{ki}y_i$ and the extinction coefficients y_i are to be obtained from the Becker–Coppens theory using the appropriate kinematical reflectivity and width parameters.

The polarization of the scattered beam is obtained from the vector sum of the scattered polarizations for each domain, each multiplied by the appropriate extinction factor and normalized by the extinguished total cross section. Identifying the nuclear, magnetic and interference contributions to the scattered polarization in the kinematical approximation given by Nunez, Brown, Forsyth & Tasset (1991) as

$$\mathbf{P}'_N = \mathbf{P}NN^*$$

$$\mathbf{P}'_M = \sum_d \alpha_d[\mathbf{Q}(\mathbf{P}\cdot\mathbf{Q}^*) + \mathbf{Q}^*(\mathbf{P}\cdot\mathbf{Q}) - \mathbf{P}(\mathbf{Q}\cdot\mathbf{Q}^*) + i(\mathbf{Q}\times\mathbf{Q}^*)]$$

$$\mathbf{P}'_I = \sum_d \alpha_d[\mathbf{Q}N^* + \mathbf{Q}^*N - i(\mathbf{P}\times\mathbf{Q}N^* - \mathbf{P}\times\mathbf{Q}^*N)]$$

and setting y_1, y_2, y_3 equal to the extinction coefficients appropriate to the three cross sections subscripted 1, 2, 3 above; the scattered polarization can be written

$$\mathbf{P}' = \{\mathbf{P}'_N y_1 + \mathbf{P}'_I[f^2 y_1 + (1-f)y_2] + \mathbf{P}'_M[f^2 y_1 + (f-f^2)y_2 + (1-f)^2 y_3]\} \times [y_1(\partial\sigma/\partial\omega)_1 + y_2(\partial\sigma/\partial\omega)_2 + y_3(\partial\sigma/\partial\omega)_3]^{-1}.$$

We have used this expression in the further treatment of the polarization analysis results.

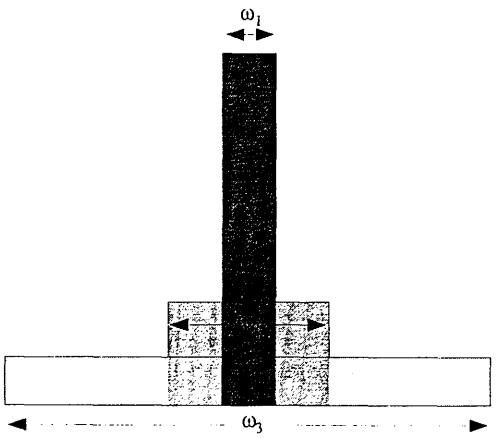

Fig. 2. A schematic representation of the reflection curve for a mixed magnetic and nuclear reflection. ω_1, ω_2 and ω_3 are the widths for nuclear, nuclear magnetic interference and magnetic scattering respectively. Different depths of shading have been used to indicate the parts of the scattered intensity to which the three different extinction factors apply.

7. Least-squares analysis of the 1.5 K integrated intensity measurements

The least-squares analysis program *MAGLSQ*, which is part of the Cambridge Crystallographic Subroutine Library (CCSL) (Matthewman, Thompson & Brown, 1982; Brown & Matthewman, 1987), has been modified to calculate reflection intensities within the model outlined above. Two extra parameters are included: a second domain radius (r_M) and the

Table 3. *Parameters of the magnetic structure of* $TbAlO_3$ *obtained from least-squares refinements based on the scattered polarizations using different extinction models*

Parameter		None	Extinction Nuclear	New model
Tb	Moment (μ_B)	11.1 (1)	12.0 (3)	8.31 (11)
	φ (°)	30 (1)	29 (1)	30.5 (6)
α_1		0.498 (5)	0.501 (5)	0.499 (3)
α_2		0.502 (5)	0.499 (5)	0.501 (3)
χ^2		12	11	7

overlap parameter f in the equations given above. The constraint $r_I^2 = r_N r_M$ has been imposed and r_N was fixed to the value found from the fit to the nuclear integrated intensities as was the mosaic spread parameter. A good fit to the integrated intensities measured at 1.5 K could be obtained, but the overlap parameter was highly correlated with the Tb moment. The Tb moment was therefore fixed to $8.25\mu_B$, the value obtained by Mareschal *et al.* (1968), and the refinement then gave the values listed in Table 2 for the remaining parameters. The extinction model seems therefore able to account for the integrated intensity measurements, but the parameters of the model cannot be determined independently from this type of measurement alone.

8. Fit of the extinction model to the measurements of scattered polarization

A program to fit the magnetic structure and extinction parameters to measurements of the scattered polarization has been written, again using the CCSL. To test the sensitivity of the results to the extinction parameters, some preliminary refinements were made first with no extinction included and then using a single domain radius fixed at that of the nuclear refinement. The results are given in Table 3. As with the 1.5 K integrated intensity measurements, assuming the same extinction (or none) for magnetic and nuclear scattering leads to an unphysically large value for the Tb magnetic moment. If, however, the extinction parameters obtained from the low-temperature integrated intensities are used as the starting values for a complete refinement, the results given in the final column of Table 3 are obtained. They can be seen to deviate somewhat from those obtained from integrated intensity measurements, but all the parameters are determined without excessive correlations. The ratio between the two domain radii r_N/r_M is 16, indicating that there are about 4000 magnetic domains in one mosaic block. All refinements gave essentially equal populations to the two 180° domains. The value 8.3(1) μ_B obtained for the magnetic moment of Tb is physically reasonable and agrees well with the results of the powder diffraction study by Mareschal *et al.* (1968). The χ^2 of 7 is somewhat larger than that obtained in the polarization refinements of CuO by Brown, Chattopadhyay, Forsyth, Nunez & Tasset (1991) and of Mn_3Sn by Brown *et al.* (1990) which has been about 4 for the same method of estimating the standard deviation of the polarization; this may be due to the fluctuations in temperature during the measurements as well as to imperfections in our extinction model.

9. Temperature dependence of the sublattice magnetization

A further check on the validity of the extinction model may be obtained from the measurements made as a function of temperature. The two reflections 112 and 140 have similar ratios γ of magnetic to nuclear structure factors 0.6 and 0.7 but they have very different nuclear structure factors 2.0 and 4.3 respectively. They should therefore have very different extinction factors and the result of this is evident from the polarization scattered when the incident polarization is parallel to the scattering vector. In both cases the presence of both types of 180° domains causes significant depolarization but for 112 the residual scattered polarization is parallel to the incident polarization whereas for the 140 reflection it is flipped. With the kinematical expressions for the polarization, spin flip cannot occur for $|\gamma| < 1$ (Nunez, Brown, Forsyth & Tasset, 1991) but in the extinction model developed above it is easy to see that spin flip will occur even with $|\gamma| < 1$ if the magnetic extinction is so much less than the nuclear extinction that the actual intensity of the magnetic scattering is greater than the nuclear.

We have used the extinction parameters derived from the full set of polarization analysis results to

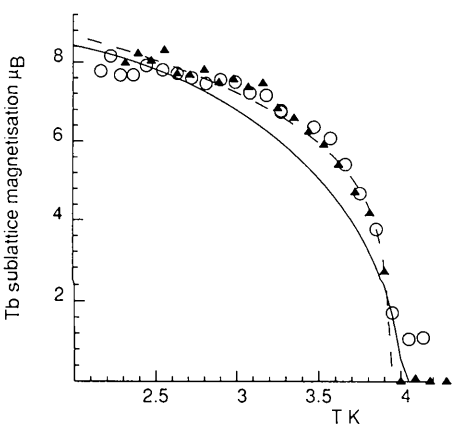

Fig. 3. Variation of the sublattice magnetization in $TbAlO_3$ as a function of temperature. The filled triangles represent values deduced from the 112 reflection and the open circles those deduced from 140. The solid line is the Brillouin function for $T_N = 4$, $S = \frac{1}{2}$ and a Landé splitting factor of 17.6; the dashed line is the function $m = m_0(1 - T/T_N)^\beta$ with $T_N = 3.93$ K and $\beta = 0.246$ (5).

calculate the temperature dependence of the sublattice magnetization from the amplitudes of the polarization scattered by the 140 and 112 reflections which were measured as a function of temperature. The results are shown in Fig. 3 where it can be seen that a very similar temperature variation is obtained from the two reflections which gives us greater confidence in the treatment of extinction.

10. Discussion

The results of this study have confirmed the magnetic structure of $TbAlO_3$ given by Mareschal *et al.* (1968). The essentially equal population of the 180° domains shows that any difference in energy between the two structures illustrated in Fig. 1 must be less than about 2×10^{-5} eV. The relative magnitudes of the domain radii for nuclear and magnetic scattering ($r_N/r_M \simeq 16$) suggests that there are about 4000 magnetic domains within each relatively perfect 'mosaic block'. Given equal energies for the 180° domains this large number accounts for the equality of the domain populations, since the statistical fluctuations with such large numbers will be small. The large number also shows that the energy of the magnetic defects associated with the 180° domain wall must also be small, since many such domain walls must be present.

We have found that the variation of the sublattice magnetization with temperature is much more rapid close to the Néel temperature than that corresponding to the Brillouin function for $J=6$. However, Wells (1970) concluded from the total entropy change in the transition that the ground state of Tb in $TbAlO_3$ is an accidental doublet and can be represented as an $s=\frac{1}{2}$ state. The full curve of Fig. 3 shows the calculated Brillouin dependence of magnetization for $s=\frac{1}{2}$, a Landé splitting factor of 17.6 and $T_N=4$ K; it can be seen that the observed magnetization falls more abruptly than the Brillouin function even with $s=\frac{1}{2}$. We have derived the critical exponent $\beta=0.246(5)$ from a least-squares fit of the temperature dependence of the magnetization with the form $m=m_0(1-T/T_N)^\beta$ and $T_N=3.93$ K: the value obtained by Wells (1970). This function is shown as the dashed curve in Fig. 3 and gives a very good fit to the data near to T_N. The value of β obtained is rather less than the $3d$ Ising result 0.312, suggesting anisotropy in the magnitude of the exchange interactions. This, rather less than three-dimensional behaviour, was also inferred by Wells (1970) from the temperature dependence of the specific heat.

Given the quite crude approximations that have been made, in particular to the shape of the reflection curve, the model which we have described seems to give quite a good account of the extinction in $TbAlO_3$. In this experiment we did not make any wavelength-dependent measurements and the discrepancy between the model parameters obtained from the integrated intensity and the polarization analysis measurements may be because they were measured at different wavelengths, 1.176 and 1.532 Å respectively. The wavelength dependence of the scattered polarizations should certainly be studied in future experiments.

This extinction model could apply to any magnetic structure in which magnetic domains can be formed at a magnetic phase transition when such formation is not accompanied by a significant lattice distortion. It is particularly applicable to magnetic structures with zero-propagation vector, since it allows the extinction in the nuclear–magnetic interference term to be calculated which cruder models, with separate nuclear and magnetic extinction, do not. It could be applicable to unmagnetized ferromagnets; but unfortunately ferromagnetic domain walls cause neutron depolarization, so only integrated intensity measurements could be used to obtain the parameters in this case. The present measurements have shown that integrated intensity measurements at a single wavelength were not able to determine all the parameters of the extinction model independently. The results of the polarization analysis, on the other hand, did enable all the parameters to be determined which illustrates once again the power of neutron polarimetry.

We are grateful to Drs M. Wells and R. C. C. Ward of the Clarendon Laboratory for their encouragement and for providing us with the crystals of $TbAlO_3$.

References

BECKER, P. & COPPENS, P. (1974). *Acta Cryst.* A**30**, 129-147.
BIDAUX, R. & MERIEL, P. (1968). *J. Phys. (Paris)*, **29**, 220-224.
BLUME, M. (1963). *Phys. Rev.* **130**, 1670-1676.
BROWN, P. J., CHATTOPADHYAY, T., FORSYTH, J. B., NUNEZ, V. & TASSET, F. (1991). *J. Phys. Condens. Matter*, **3**, 4281-4287.
BROWN, P. J. & MATTHEWMAN, J. C. (1987). Report RAL-87-010. Rutherford Appleton Laboratory, Chilton, England.
BROWN, P. J., NUNEZ, V., TASSET, F., FORSYTH, J. B. & RADHAKRISHNA, P. (1990). *J. Phys. Condens. Matter*, **2**, 9409-9422.
COX, D. E. (1974). *Int. J. Magn.* **6**, 67-75.
FREEMAN, A. J. & DESCLAUX, J. P. (1979). *J. Magn. Magn. Mater.* **12**, 11-21.
MARESCHAL, J., SIVARDIÈRE, J., DE VRIES, G. F. & BERTAUT, E. E. (1968). *J. Appl. Phys.* **39**, 1364-1366.
MATTHEWMAN, J. C., THOMPSON, P. & BROWN, P. J. (1982). *J. Appl. Cryst.* **15**, 167-173.
MERCIER, M. & CURSOUX, B. (1968). *Solid State Commum.* **6**, 207-209.
NUNEZ, V., BROWN, P. J., FORSYTH, J. B. & TASSET, F. (1991). *Physica (Utrecht)*, B**174**, 60-65.
TASSET, F. (1989). *Physica (Utrecht)*, B**156–157**, 627-630.
TASSET, F., BROWN, P. J. & FORSYTH, J. B. (1988). *J. Appl. Phys.* **63**, 3606-3608.
WELLS, M. (1970). DPhil thesis, Univ. of Oxford, England.